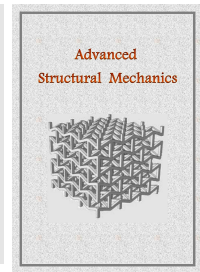


Advanced Structural Mechanics

Journal homepage: <http://asm.sku.ac.ir>



Free vibration analysis of piezoelectric nanotube conveying fluid supported by a visco-Pasternak foundation

Forough Kheibari^a, Yaghoub Tadi Beni^{b, c*}

^aDepartment of Mechanical Engineering, Shahrekord University, Shahrekord, Iran

^bFaculty of Engineering, Shahrekord University, Shahrekord, Iran

^cNanotechnology Research Institute, Shahrekord, University, Shahrekord, Iran

Article received: 2023/05/11, Article revised: 2023/09/08, Article accepted: 2023/09/09

ABSTRACT

In the concept of sensor and actuator applications, sensing and actuating in small scales that have nowadays a wide range of engineering applications are of paramount importance and interest. Some of these sensors and actuators must work in the presence of other materials like fluids. In this paper, free vibration analysis of piezoelectric nanotube conveying fluid and resting on the visco-Pasternak foundation is performed. The displacement field is based on the first-order shear deformation theory, and the modified couple stress theory is utilized for consideration of nanoscale size effects. The closed-form Navier solution is considered for simply supported piezoelectric fluid conveying nanotubes, and finally, the governing equations are derived according to the Hamilton principle. The results are compared with other results found in the literature and a good agreement is achieved. The effects of various parameters such as fluid velocity, size effect parameter, geometry of nanotube, and visco-Pasternak foundation on the natural frequency and damping of fluid conveying nanotube are investigated

Keywords: Piezoelectric; couple stress theory; fluid conveying nanotube; free vibration.

Introduction

Piezoelectric materials have very important properties making them very applicable in engineering fields such as sensors and actuators. Piezoelectric materials respond to mechanical loads by producing electric voltage. Moreover, they respond by mechanical deformations to the electric voltage imposed on them.

In the concept of sensor and actuator applications, it is very interesting and important to sense and actuate in small scales that nowadays have a wide range of engineering applications. Nano electro-mechanical systems (NEMS) are systems constructed by compounds of mechanical and electrical components on very small scales that work as a unit to attain a goal. Piezoelectric materials can be used on small scales in NEMS for special applications

* Corresponding author at: Faculty of Engineering, Shahrekord University, Shahrekord, Iran.

E-mail address: tadi@sku.ac.ir

DOI: 10.22034/asm.2023.14390.1013: https://asm.sku.ac.ir/article_11508.html

as sensors and actuators. Therefore, it seems that studying the coupled mechanical and electrical responses of piezoelectric materials is very critical to predicting their performance in NEMS. Recently micro/nano structures with or without fluid flow are widely used by many researchers, some examples can be seen in ref [1-6]. For understanding a more accurate mechanical response of nanotubes, it seems that the shell models should be used instead of beam models. Various nanoshell models are widely used in nanodevices such as electromechanical nanosystems, sensors, drug delivery, and electricity conduction in electronic nanodevices [7-9]. In this regard, Yin et al. [10] investigated vibrations of micro beams conveying fluid by couple stress theory and concluded that the natural frequencies of micro beams decrease by increasing the fluid density. Ghorbanpourarani et al. [11], studied vibrations of single-wall and double-wall nanotubes, they used both beams and shell theories, i.e., Timoshenko and Euler-Bernoulli beam theories and Donnell shell theory in their work. They concluded that the natural frequencies predicted by shell models are higher than those of beam models. Xinpeng and Lin [12] studied vibration analysis of a micro shell conveying fluid by couple stress theory and concluded that changing the fluid velocity affects the stability of the micro-shell. Alibaigloo and Shaban conducted a free vibration analysis of single-wall carbon nanotubes according to three-dimensional nonlocal elasticity theory [13]. Zeighampour and Tadi Beni [14] investigated the free vibration of single-wall conical nanoshells based on couple stress theory. Tadi Beni et al., conducted a free vibration analysis of size-dependent shear deformable functionally graded cylindrical shell based on modified couple stress theory [15]. Zeighampour and Tadi Beni [16] studied free vibration analysis of cylindrical shells via cylindrical thin-shell model based on modified strain gradient theory. Bahaadini et al. [17], investigated nonlocal and surface effects on the flutter instability of cantilevered nanotubes conveying fluid subjected to follower forces. Piezoelectric nanostructures are structures whose dimensions vary from hundreds of nanometers to nanometers. In this dimension, the size effects are very important and play a significant role in their structural analysis. The size-dependent property of piezoelectric materials was observed in atomistic tests and simulations [18-20], so the size effects should be included in theoretical and experimental studies of piezoelectric nanostructures. Some studies on piezoelectric micro/nanostructures are as follows:

Ke et al. [21], performed thermo-electro-mechanical vibration of size-dependent piezoelectric cylindrical nanoshells under various boundary conditions. They used nonlocal elasticity theory and evaluated the effects of temperature, electric voltage, and radius-to-thickness ratio on natural frequencies. Kheibari and Tadi Beni studied the size-dependent electro-mechanical vibration of single-walled piezoelectric nanotubes using a thin shell model [22]. They used both size-dependent piezoelectric theory and classical continuum theory and concluded that the natural frequencies increase by increasing the size effect.

Free vibration analysis of piezoelectric nanotube conveying fluid resting on a visco-Pasternak foundation has not been conducted yet. Therefore, the present study aims to conduct a free vibration analysis of piezoelectric nanotube conveying fluid based on the first-order shear deformation theory of shells. To improve the size effect, modified couple stress theory is used. The Navier solution is considered for simply supported end conditions and effects of various parameters such as foundation coefficients, fluid parameters, etc., on the natural frequencies and damping parameters of the system are investigated.

1. Problem description

A fluid-conveying nanoshell with radius R , length L , and thickness h , is shown in its cylindrical coordinate system in Fig. 1. The displacement components U , V and W are introduced in x , θ and z directions of the nanoshell, respectively. The outer surface of the nanotube is rested on a visco-Pasternak foundation with the Pasternak constant k_g , Winkler constant k_w , and damping coefficient C_d .

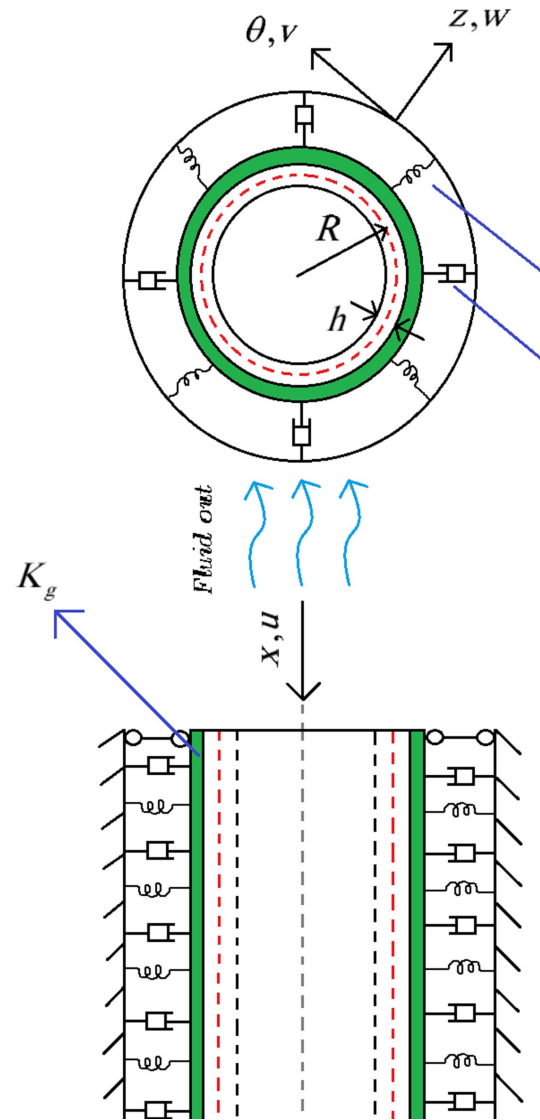


Fig.1. Geometry and coordinate system of nanoshell.

1.2 Constitutive equations

The general coupled constitutive relations for a piezoelectric medium are as follows:

$$\sigma_{ij} = c_{ijkl} \varepsilon_{kl} - e_{mij} E_m \quad (1)$$

And,

$$D_i = e_{ikl} \varepsilon_{kl} + s_{im} E_m \quad (2)$$

By considering the size effect with the modified couple stress theory, another constitutive relation for a nanoscale body is as follows:

$$m_{ij} = 2l^2 \mu \chi_{ij}^s \quad (3)$$

Where in Eqs. (1) - (3), σ_{ij} , D_i and m_{ij} are components of the stress tensor, electric displacement vector, and couple stress tensor, respectively, and ε_{ij} , E_i and χ_{ij} are the components of the strain tensor, electric field vector, and rotation gradient tensor, respectively that are defined as:

$$\varepsilon_{ij} = \frac{1}{2} (u_{i,j} + u_{j,i}) \quad (4)$$

$$\chi_{ij} = \omega_{i,j} = \frac{1}{4} (e_{ipq} \eta_{jpq} + e_{j pq} \eta_{ipq}) \quad (5)$$

$$E_i = -\phi_{,i} \quad (6)$$

Where u_i , η_{ipq} and e_{ipq} are displacement vector components, permutation symbol, and strain gradient tensor, respectively.

The relation between stresses and strains for piezoelectric cylindrical shell in the plane stress condition is defined as:

$$\begin{Bmatrix} \sigma_{xx} \\ \sigma_{\theta\theta} \\ \sigma_{x\theta} \\ \sigma_{\theta z} \\ \sigma_{xz} \end{Bmatrix} = \begin{bmatrix} \tilde{c}_{11} & \tilde{c}_{12} & 0 & 0 & 0 \\ \tilde{c}_{12} & \tilde{c}_{22} & 0 & 0 & 0 \\ 0 & 0 & \tilde{c}_{66} & 0 & 0 \\ 0 & 0 & 0 & \tilde{c}_{44} & 0 \\ 0 & 0 & 0 & 0 & \tilde{c}_{55} \end{bmatrix} \begin{Bmatrix} \varepsilon_{xx} \\ \varepsilon_{\theta\theta} \\ \varepsilon_{x\theta} \\ \varepsilon_{\theta z} \\ \varepsilon_{xz} \end{Bmatrix} - \begin{bmatrix} 0 & 0 & \tilde{e}_{31} \\ 0 & 0 & \tilde{e}_{332} \\ 0 & 0 & 0 \\ 0 & \tilde{e}_{24} & 0 \\ \tilde{e}_{15} & 0 & 0 \end{bmatrix} \begin{Bmatrix} E_x \\ E_\theta \\ E_z \end{Bmatrix} \quad (7)$$

$$\begin{Bmatrix} D_x \\ D_\theta \\ D_z \end{Bmatrix} = \begin{bmatrix} 0 & 0 & 0 & 0 & \tilde{e}_{15} \\ 0 & 0 & 0 & \tilde{e}_{24} & 0 \\ \tilde{e}_{31} & \tilde{e}_{32} & 0 & 0 & 0 \end{bmatrix} \begin{Bmatrix} \varepsilon_{xx} \\ \varepsilon_{\theta\theta} \\ \gamma_{x\theta} \\ \gamma_{\theta z} \\ \gamma_{xz} \end{Bmatrix} + \begin{bmatrix} \tilde{s}_{11} & 0 & 0 \\ 0 & \tilde{s}_{22} & 0 \\ 0 & 0 & \tilde{s}_{33} \end{bmatrix} \begin{Bmatrix} E_x \\ E_\theta \\ E_z \end{Bmatrix} \quad (8)$$

In which c_{ij} , \tilde{e}_{ij} and \tilde{s}_{ij} are decreased elastic constant components, piezoelectric and dielectric constants, respectively, defined as:

$$\begin{aligned}
\tilde{c}_{11} &= c_{11} - \frac{c_{13}^2}{c_{33}}, \quad \tilde{c}_{12} = c_{12} - \frac{c_{13}c_{23}}{c_{33}}, \quad \tilde{c}_{22} = c_{22} - \frac{c_{23}^2}{c_{33}}, \quad \tilde{c}_{44} = c_{44}, \quad \tilde{c}_{55} = c_{55}, \quad \tilde{c}_{66} = c_{66}, \\
\tilde{e}_{31} &= e_{31} - \frac{c_{13}e_{33}}{c_{33}}, \quad \tilde{e}_{32} = e_{32} - \frac{c_{23}e_{33}}{c_{33}}, \quad \tilde{e}_{24} = e_{24}, \quad \tilde{e}_{15} = e_{15}, \\
\tilde{s}_{11} &= s_{11}, \quad \tilde{s}_{22} = s_{22}, \quad \tilde{s}_{33} = s_{33} + \frac{e_{33}^2}{c_{33}}
\end{aligned} \tag{9}$$

1.3. Displacement and electric fields by first-order shear deformation theory

According to the first-order shear deformation theory, the displacement field for nanoshells is considered as:

$$\begin{aligned}
u(x, \theta, z, t) &= U(x, \theta, t) + z\psi_x(x, \theta, t), \\
v(x, \theta, z, t) &= V(x, \theta, t) + z\psi_\theta(x, \theta, t), \\
w(x, \theta, z, t) &= W(x, \theta, t).
\end{aligned} \tag{10}$$

Where u , v and w are displacement components in x , θ and z directions, respectively. Here the displacement components at the mid surface of the nanoshell are introduced by $U(x, \theta, t)$, $V(x, \theta, t)$ and $W(x, \theta, t)$. Moreover, in the above equations, t denote the time and $\psi_x(x, \theta, t)$ and $\psi_\theta(x, \theta, t)$ are normal rotations about lateral and axial axes.

Wang et al., [21] proposed a model for electric potential as a combination of a cosine and a linear function of z and an unknown function of other two coordinates and time as follows:

$$\phi(x, \theta, z, t) = -\cos(\beta z)\varphi(x, \theta, t) + \frac{2z\varphi_0}{h}. \tag{11}$$

Where $\beta = \frac{\pi}{h}$ and $\varphi(x, \theta, t)$ is an unknown function to be determined. In addition, φ_0 is the potential difference applied between the inner and outer surface of the nanoshell.

The strain–displacement relations in cylindrical coordinates are introduced below:

$$\begin{aligned}
e_{zz} &= \frac{\partial w}{\partial z}, \quad e_{\theta\theta} = \frac{1}{R(1+z/R)} \left[\frac{\partial v}{\partial \theta} + w \right], \\
e_{xx} &= \frac{\partial u}{\partial x}, \quad e_{zx} = e_{xz} = \frac{1}{2} \left[\frac{\partial w}{\partial x} + \frac{\partial u}{\partial z} \right], \\
e_{z\theta} &= e_{\theta z} = \frac{1}{2} \left[\frac{1}{R(1+z/R)} \frac{\partial w}{\partial \theta} + \frac{\partial v}{\partial z} - \frac{v}{R(1+z/R)} \right], \\
e_{x\theta} &= e_{\theta x} = \frac{1}{2} \left[\frac{1}{R(1+z/R)} \frac{\partial u}{\partial \theta} + \frac{\partial v}{\partial x} \right].
\end{aligned} \tag{12}$$

Also, the nonzero components of strain gradient have the following relations with displacement components:

$$\begin{aligned}
\eta_{xx} &= \frac{\partial^2 u}{\partial x^2}, \quad \eta_{xx\theta} = \frac{\partial^2 v}{\partial x^2}, \quad \eta_{zx\theta} = \eta_{xz\theta} = \frac{\partial^2 v}{\partial x \partial z}, \quad \eta_{zz\theta} = \frac{\partial^2 v}{\partial z^2}, \quad \eta_{xxz} = \frac{\partial^2 w}{\partial x^2}, \quad \eta_{xxz} = \frac{\partial^2 u}{\partial x \partial z}, \\
\eta_{zzz} &= \frac{\partial^2 w}{\partial z^2}, \quad \eta_{zzx} = \frac{\partial^2 u}{\partial z^2}, \quad \eta_{zzz} = \eta_{zzz} = \frac{\partial^2 w}{\partial x \partial z}, \quad \eta_{x\theta\theta} = \eta_{\theta z\theta} = \frac{1}{R(1+z/R)} \left[\frac{\partial^2 v}{\partial x \partial \theta} + \frac{\partial w}{\partial x} \right], \\
\eta_{\theta xx} &= \eta_{x\theta x} = \frac{1}{R(1+z/R)} \frac{\partial^2 u}{\partial x \partial \theta}, \quad \eta_{\theta\theta x} = \frac{1}{R(1+z/R)} \left[\frac{1}{R(1+z/R)} \frac{\partial^2 u}{\partial \theta^2} + \frac{\partial u}{\partial z} \right], \\
\eta_{\theta\theta\theta} &= \frac{1}{(R(1+z/R))^2} \left[\frac{\partial^2 v}{\partial \theta^2} + 2 \frac{\partial w}{\partial \theta} + R(1+z/R) \frac{\partial v}{\partial z} - v \right], \\
\eta_{\theta\theta z} &= \frac{1}{(R(1+z/R))^2} \left[\frac{\partial^2 w}{\partial \theta^2} - 2 \frac{\partial v}{\partial \theta} + R(1+z/R) \frac{\partial v}{\partial z} - w \right], \\
\eta_{z\theta\theta} &= \eta_{\theta z\theta} = \frac{1}{R(1+z/R)} \left[\frac{\partial^2 v}{\partial z \partial \theta} - \frac{1}{R(1+z/R)} \frac{\partial v}{\partial \theta} + \frac{\partial w}{\partial z} - \frac{w}{R(1+z/R)} \right], \\
\eta_{z\theta z} &= \eta_{\theta z z} = \frac{1}{R(1+z/R)} \left[\frac{\partial^2 w}{\partial z \partial \theta} - \frac{1}{R(1+z/R)} \frac{\partial w}{\partial \theta} - \frac{\partial v}{\partial z} + \frac{v}{R(1+z/R)} \right], \\
\eta_{z\theta x} &= \eta_{\theta z x} = \frac{1}{R(1+z/R)} \left[\frac{\partial^2 u}{\partial z \partial \theta} - \frac{1}{R(1+z/R)} \frac{\partial u}{\partial \theta} \right], \\
\eta_{x\theta z} &= \eta_{\theta x z} = \frac{1}{R(1+z/R)} \left[\frac{\partial^2 w}{\partial x \partial \theta} - \frac{\partial v}{\partial x} \right].
\end{aligned} \tag{13}$$

And the components of the electric field vector are defined as:

$$\begin{aligned}
E_x &= -\frac{\partial \phi}{\partial x}, \\
E_\theta &= -\frac{1}{R} \frac{\partial \phi}{\partial \theta}, \\
E_z &= -\frac{\partial \phi}{\partial z}.
\end{aligned} \tag{14}$$

By substituting Eq. (10) into Eqs. (12) and (13), and Eq. (11) into Eq. (14), the nonzero components of classic strain, nonclassic strain, and electric field for piezoelectric nanoshell based on the first-order shear deformation theory, are derived as follow:

$$\begin{aligned}
\varepsilon_{xx} &= \frac{\partial U}{\partial x} + z \frac{\partial \psi_x}{\partial x}, \\
\varepsilon_{\theta\theta} &= \frac{1}{R} \left[\frac{\partial V}{\partial \theta} + W \right], \\
\gamma_{x\theta} &= \frac{\partial V}{\partial x} + z \frac{\partial \psi_\theta}{\partial x} + \frac{1}{R} \frac{\partial U}{\partial \theta}, \\
\gamma_{xz} &= \frac{\partial W}{\partial x} + \psi_x, \\
\gamma_{\theta z} &= \psi_\theta + \frac{1}{R} \frac{\partial W}{\partial \theta} - \frac{V}{R}.
\end{aligned} \tag{15}$$

$$\begin{aligned}
\chi_{xx} &= \frac{1}{2R} \frac{\partial^2 W}{\partial x \partial \theta} - \frac{1}{2R} \frac{\partial V}{\partial x} - \frac{1}{2} \frac{\partial \psi_\theta}{\partial x}, \\
\chi_{\theta\theta} &= -\frac{1}{2R} \frac{\partial^2 W}{\partial x \partial \theta} - \frac{1}{2R^2} \frac{\partial U}{\partial \theta} + \frac{1}{2R} \frac{\partial \psi_x}{\partial \theta} + \frac{1}{2R} \frac{\partial V}{\partial x}, \\
\chi_{zz} &= \frac{1}{2} \frac{\partial \psi_\theta}{\partial x} - \frac{1}{2R} \frac{\partial \psi_x}{\partial \theta} + \frac{1}{2R^2} \frac{\partial U}{\partial \theta}, \\
\chi_{x\theta} &= \chi_{\theta x} = \frac{1}{4R^2} \frac{\partial^2 W}{\partial \theta^2} - \frac{1}{4R^2} \frac{\partial V}{\partial \theta} - \frac{1}{4} \frac{\partial^2 W}{\partial x^2} - \frac{1}{4R} \frac{\partial \psi_\theta}{\partial \theta} + \frac{1}{4} \frac{\partial \psi_x}{\partial x}, \\
\chi_{xz} &= \chi_{zx} = \frac{1}{4} \frac{\partial^2 V}{\partial x^2} + \frac{z}{4} \frac{\partial^2 \psi_\theta}{\partial x^2} - \frac{1}{4R^2} \frac{\partial W}{\partial \theta} - \frac{1}{4R} \psi_\theta + \frac{1}{4R^2} V - \frac{1}{4R} \frac{\partial^2 U}{\partial x \partial \theta}, \\
\chi_{z\theta} &= \chi_{\theta z} = \frac{1}{4R} \frac{\partial^2 V}{\partial x \partial \theta} + \frac{1}{4R} \frac{\partial W}{\partial x} - \frac{1}{4R^2} \frac{\partial^2 U}{\partial \theta^2} - \frac{1}{4R} \psi_x.
\end{aligned} \tag{16}$$

$$\begin{aligned}
E_x &= \cos(\beta z) \frac{\partial \phi}{\partial x}, \\
E_\theta &= \frac{\cos(\beta z)}{R} \frac{\partial \phi}{\partial \theta}, \\
E_z &= -\beta \sin(\beta z) \phi - \frac{2\phi_0}{h}.
\end{aligned} \tag{17}$$

The above relations are derived according to thin shell theory considerations, these conditions are:

$$\begin{aligned}
1 + z/R &\approx 1 \\
(z/R)^2 &\approx 0.
\end{aligned} \tag{18}$$

2.2. Hamilton principal

The Hamilton principle for the present problem that contains all energy sources is as follows:

$$\int_{t_1}^{t_2} (\delta T - \delta U + \delta W_f + \delta W_{ef} - \dot{\delta} D) dt = 0. \quad (19)$$

Where T , U and D are kinetic, potential, and damping energy, respectively that are defined as follows:

$$T = \frac{1}{2} \rho_t \int_0^{2\pi} \int_0^L \int_{-h/2}^{h/2} \left\{ \left(\frac{\partial U}{\partial t} + z \frac{\partial \psi_x}{\partial t} \right)^2 + \left(\frac{\partial V}{\partial t} + z \frac{\partial \psi_\theta}{\partial t} \right)^2 + \left(\frac{\partial W}{\partial t} \right)^2 \right\} R dx d\theta dz. \quad (20)$$

$$U = \frac{1}{2} \int_{\Omega} (\sigma_{ij} \varepsilon_{ij} + m_{ij}^s \chi_{ij}^s - D_i E_i) dV \quad (21)$$

$$D = \frac{1}{2} \int_0^{2\pi} \int_0^L C_d \left(\frac{\partial W}{\partial t} \right)^2 R dx d\theta. \quad (22)$$

Where ρ_t and C_d are the mass density of the nanoshell and damping coefficient, respectively. Also W_f and W_{ef} are the works done by non-viscous fluid and Pasternak foundation forces.

The work done by a nonviscous fluid is derived from Navier- stokes equations:

$$W_f = \int_0^{2\pi} \int_0^L \left\{ -\frac{\rho_f R}{2} \left(\frac{\partial^2 W}{\partial t^2} + 2\nu_F \frac{\partial^2 W}{\partial x \partial t} + \nu_F^2 \frac{\partial^2 W}{\partial x^2} \right) \right\} R dx d\theta. \quad (23)$$

$$W_f = \int_0^{2\pi} \int_0^L \left\{ -\frac{\rho_f R}{2} \left(\frac{\partial^2 W}{\partial t^2} + 2\nu_F \frac{\partial^2 W}{\partial x \partial t} + \nu_F^2 \frac{\partial^2 W}{\partial x^2} \right) \right\} R dx d\theta.$$

Pasternak foundation work is defined as:

$$W_{ef} = \frac{1}{2} \int_0^{2\pi} \int_0^L (-k_w W + k_g \nabla^2 W) W R dx d\theta, \quad (24)$$

$$\nabla^2 = \frac{\partial^2}{\partial x^2} + \frac{1}{R^2} \frac{\partial^2}{\partial \theta^2}.$$

In the above equations, ν_f and ρ_f are the fluid velocity and the fluid density. k_g And k_w are Winkler constant and Pasternak constant, respectively.

Substitution of Eqs. (7), (8) and (15)-(17) into Eq. (19) gives the potential energy of piezoelectric nanoshell based on resultant force and moments as:

$$\begin{aligned}
\bar{U}_s = & \frac{1}{2} \int_{\Omega} \left(\sigma_{ij} \varepsilon_{ij} + m_{ij} \chi_{ij} - D_i E_i \right) dV = \frac{1}{2} \int_0^{2\pi} \int_0^L \left[(N_{xx}) \frac{\partial U}{\partial x} + \left(\frac{N_{x\theta}}{R} - \frac{Y_{\theta\theta}}{2R^2} + \frac{Y_{zz}}{2R^2} \right) \frac{\partial U}{\partial \theta} - \right. \\
& \left(\frac{Y_{\theta z}}{2R^2} \right) \frac{\partial^2 U}{\partial \theta^2} - \left(\frac{Y_{xz}}{2R} \right) \frac{\partial^2 U}{\partial x \partial \theta} + \left(N_{x\theta} + \frac{Y_{\theta\theta}}{2R} - \frac{Y_{xx}}{2R} \right) \frac{\partial V}{\partial x} + \left(\frac{T_{xz}}{2R^2} - \frac{Q_{z\theta}}{R} \right) V + \\
& \left(\frac{N_{\theta\theta}}{R} - \frac{Y_{x\theta}}{2R^2} \right) \frac{\partial V}{\partial \theta} + \left(\frac{Y_{xz}}{2} \right) \frac{\partial^2 V}{\partial x^2} + \left(\frac{Y_{\theta z}}{2R} \right) \frac{\partial^2 V}{\partial x \partial \theta} + \left(\frac{N_{\theta\theta}}{R} \right) W + \left(Q_{xz} + \frac{Y_{\theta z}}{2R} \right) \frac{\partial W}{\partial x} + \\
& \left(\frac{Y_{x\theta}}{2} \right) \frac{\partial^2 W}{\partial x^2} + \left(\frac{Q_{z\theta}}{R} - \frac{T_{xz}}{2R^2} \right) \frac{\partial W}{\partial \theta} + \left(\frac{Y_{x\theta}}{2R^2} \right) \frac{\partial^2 W}{\partial \theta^2} + \left(\frac{Y_{xx}}{2R} - \frac{Y_{\theta\theta}}{2R} \right) \frac{\partial^2 W}{\partial x \partial \theta} + \\
& \left(Q_{xz} - \frac{Y_{\theta z}}{2R} \right) \psi_x + \left(M_{xx} + M_{x\theta} + \frac{Y_{x\theta}}{2} \right) \frac{\partial \psi_x}{\partial x} + \left(\frac{M_{x\theta}}{R} + \frac{Y_{\theta\theta}}{2R} - \frac{T_{\theta\theta}}{2R^2} + \frac{T_{zz}}{2R^2} - \frac{Y_{zz}}{2R} \right) \frac{\partial \psi_x}{\partial \theta} \\
& - \left(\frac{T_{xz}}{2R^2} \right) \frac{\partial^2 \psi_x}{\partial x \partial \theta} - \left(\frac{T_{\theta z}}{2R^2} \right) \frac{\partial^2 \psi_x}{\partial \theta^2} + \left(Q_{z\theta} - \frac{Y_{xz}}{2R} \right) \psi_{\theta} + \left(-\frac{Y_{xx}}{2} + \frac{T_{\theta\theta}}{2R} + \frac{Y_{zz}}{2} \right) \frac{\partial \psi_{\theta}}{\partial x} + \\
& \left(\frac{M_{\theta\theta}}{R} - \frac{Y_{x\theta}}{2R} - \frac{T_{x\theta}}{2R^2} \right) \frac{\partial \psi_{\theta}}{\partial \theta} + \left(\frac{T_{\theta z}}{2R} \right) \frac{\partial^2 \psi_{\theta}}{\partial x \partial \theta} - \int_{-h/2}^{h/2} (D_x E_x + D_{\theta} E_{\theta} + D_z E_z)] R dx d\theta
\end{aligned} \tag{25}$$

Where classical and nonclassical resultant forces and moments are defined as follows:

$$(N_{xx}, N_{\theta\theta}, N_{x\theta}) = \int_{-h/2}^{h/2} (\sigma_{xx}, \sigma_{\theta\theta}, \sigma_{x\theta}) dz \tag{26}$$

$$(M_{xx}, M_{\theta\theta}, M_{x\theta}) = \int_{-h/2}^{h/2} (\sigma_{xx}, \sigma_{\theta\theta}, \sigma_{x\theta}) z dz \tag{27}$$

$$(Q_{xz}, Q_{z\theta}) = \int_{-h/2}^{h/2} (\sigma_{xz}, \sigma_{z\theta}) dz \tag{28}$$

$$(Y_{xx}, Y_{\theta\theta}, Y_{zz}, Y_{x\theta}, Y_{xz}, Y_{z\theta}) = \int_{-h/2}^{h/2} (m_{xx}, m_{\theta\theta}, m_{zz}, m_{x\theta}, m_{xz}, m_{z\theta}) dz \tag{29}$$

$$(T_{xx}, T_{\theta\theta}, T_{zz}, T_{x\theta}, T_{xz}, T_{z\theta}) = \int_{-h/2}^{h/2} (m_{xx}, m_{\theta\theta}, m_{zz}, m_{x\theta}, m_{xz}, m_{z\theta}) z dz \tag{30}$$

By substituting Eqs. (20)- (25) Into Eq. (19) and using the variation principles, the equations of motion governed by the free vibration of piezoelectric nanoshell are derived as follows:

$$\begin{aligned}
\delta U : & A_1 \frac{\partial^4 U}{\partial \theta^4} + A_2 \frac{\partial^4 V}{\partial x \partial \theta^3} + A_3 \frac{\partial^3 W}{\partial x \partial \theta^2} + A_4 \frac{\partial^2 \psi_x}{\partial \theta^2} + A_5 \frac{\partial^2 \psi_{\theta}}{\partial x \partial \theta} + A_6 \frac{\partial^2 U}{\partial \theta^2} + A_7 \frac{\partial^2 U}{\partial x^2} + \\
& A_8 \frac{\partial^2 V}{\partial x \partial \theta} + A_9 \frac{\partial W}{\partial x} + A_{10} \frac{\partial^2 U}{\partial t^2} = 0,
\end{aligned} \tag{31}$$

$$\begin{aligned}
\delta V: & B_1 \frac{\partial^3 W}{\partial x^2 \partial \theta} + B_2 \frac{\partial^2 V}{\partial x^2} + B_3 \frac{\partial^2 \psi_\theta}{\partial x^2} + B_4 \frac{\partial^3 W}{\partial \theta^3} + B_5 \frac{\partial^2 V}{\partial \theta^2} + B_6 \frac{\partial^2 \psi_\theta}{\partial \theta^2} + B_7 \frac{\partial^2 \psi_x}{\partial x \partial \theta} + \\
& B_8 \frac{\partial W}{\partial \theta} + B_9 \psi_\theta + B_{10} V + B_{11} \frac{\partial^2 U}{\partial x \partial \theta} + B_{12} \frac{\partial^4 V}{\partial x^4} + B_{13} \frac{\partial^4 U}{\partial x^3 \partial \theta} + B_{14} \frac{\partial^4 V}{\partial x^2 \partial \theta^2} + B_{15} \frac{\partial^4 U}{\partial x \partial \theta^3} \\
& + B_{16} \frac{\partial \phi}{\partial \theta} + B_{17} \frac{\partial^2 U}{\partial t^2} = 0
\end{aligned} \tag{32}$$

$$\begin{aligned}
\delta W: & E_1 \frac{\partial^4 W}{\partial x^2 \partial \theta^2} + E_2 \frac{\partial^3 V}{\partial x^2 \partial \theta} + E_3 \frac{\partial^3 \psi_\theta}{\partial x^2 \partial \theta} + E_4 \frac{\partial^4 W}{\partial \theta^4} + E_5 \frac{\partial^3 V}{\partial \theta^3} + E_6 \frac{\partial^3 \psi_\theta}{\partial \theta^3} + E_7 \frac{\partial^3 \psi_x}{\partial x \partial \theta^2} + \\
& E_8 \frac{\partial^4 W}{\partial x^4} + E_9 \frac{\partial^3 \psi_x}{\partial x^3} + E_{10} \frac{\partial^2 W}{\partial \theta^2} + E_{11} \frac{\partial \psi_\theta}{\partial \theta} + E_{12} \frac{\partial V}{\partial \theta} + E_{13} \frac{\partial^3 U}{\partial x \partial \theta^2} + E_{14} \frac{\partial^2 W}{\partial x^2} + E_{15} \frac{\partial \psi_x}{\partial x} + \\
& E_{16} \frac{\partial U}{\partial x} + E_{17} W + E_{18} \frac{\partial^2 \phi}{\partial \theta^2} + E_{19} \frac{\partial^2 \phi}{\partial x^2} + E_{20} + E_{21} \frac{\partial^2 W}{\partial x \partial t} + E_{22} \frac{\partial W}{\partial t} + E_{23} \frac{\partial^2 W}{\partial t^2} = 0
\end{aligned} \tag{33}$$

$$\begin{aligned}
\delta \psi_x: & C_1 \frac{\partial^3 W}{\partial x \partial \theta^2} + C_2 \frac{\partial^2 V}{\partial x \partial \theta} + C_3 \frac{\partial^2 \psi_\theta}{\partial x \partial \theta} + C_4 \frac{\partial^3 W}{\partial x^3} + C_5 \frac{\partial^2 \psi_x}{\partial x^2} + C_6 \frac{\partial^2 \psi_x}{\partial \theta^2} + \\
& C_7 \frac{\partial^2 U}{\partial \theta^2} + C_8 \frac{\partial W}{\partial x} + C_9 \psi_x + C_{10} \frac{\partial \phi}{\partial x} + C_{11} \frac{\partial^2 \psi_x}{\partial t^2} = 0
\end{aligned} \tag{34}$$

$$\begin{aligned}
\delta \psi_\theta: & D_1 \frac{\partial^3 W}{\partial x^2 \partial \theta} + D_2 \frac{\partial^2 V}{\partial x^2} + D_3 \frac{\partial^2 \psi_\theta}{\partial x^2} + D_4 \frac{\partial^3 W}{\partial \theta^3} + D_5 \frac{\partial^2 V}{\partial \theta^2} + D_6 \frac{\partial^2 \psi_\theta}{\partial \theta^2} + D_7 \frac{\partial^2 \psi_x}{\partial x \partial \theta} + \\
& D_8 \frac{\partial W}{\partial \theta} + D_9 \psi_\theta + D_{10} V + D_{11} \frac{\partial^2 U}{\partial x \partial \theta} + D_{12} \frac{\partial^4 \psi_\theta}{\partial x^4} + D_{13} \frac{\partial \phi}{\partial \theta} + D_{14} \frac{\partial^2 \psi_\theta}{\partial t^2} = 0
\end{aligned} \tag{35}$$

$$\delta \phi: F_1 \frac{\partial \psi_x}{\partial x} + F_2 \frac{\partial \psi_\theta}{\partial \theta} + F_3 \frac{\partial^2 W}{\partial \theta^2} + F_4 \frac{\partial V}{\partial \theta} + F_5 \frac{\partial^2 W}{\partial x^2} + F_6 \frac{\partial^2 \phi}{\partial x^2} + F_7 \frac{\partial^2 \phi}{\partial \theta^2} + F_8 \phi = 0 \tag{36}$$

The coefficients $A_i, B_i, C_i, D_i, E_i, F_i$ are presented in Appendix A.

The boundary conditions in the constant x case are as follow:

$$\int_0^{2\pi} (\tilde{c}_{11} h \frac{\partial U}{\partial x} + \left(\frac{l^2 \mu h}{4R^3} + \frac{\tilde{c}_{12} h}{R} \right) \frac{\partial V}{\partial \theta} + \frac{l^2 \mu h}{4R} \frac{\partial^3 V}{\partial \theta \partial x^2} - \frac{l^2 \mu h}{4R^3} \frac{\partial^2 W}{\partial \theta^2} - \frac{l^2 \mu h}{4R^2} \frac{\partial \psi_\theta}{\partial \theta} - \frac{l^2 \mu h}{4R^2} \frac{\partial^3 U}{\partial \theta^2 \partial x} + \frac{\tilde{c}_{12} h}{R} W) R d\theta \Big|_0^L = 0 \quad \text{Or} \quad \delta U \Big|_{x=0,L} = 0, \quad (37)$$

$$\int_0^{2\pi} \left(\left(\frac{\tilde{c}_{66} h}{4R} - \frac{l^2 \mu h}{2R^3} \right) \frac{\partial U}{\partial \theta} + \left(\frac{3l^2 \mu h}{4R^2} + \frac{\tilde{c}_{66} h}{4} \right) \frac{\partial V}{\partial x} - \frac{l^2 \mu h}{4R^2} \frac{\partial^3 V}{\partial x \partial \theta^2} - \frac{l^2 \mu h}{R^2} \frac{\partial^2 W}{\partial x \partial \theta} + \frac{3l^2 \mu h}{4R^2} \frac{\partial \psi_x}{\partial \theta} + \frac{l^2 \mu h}{4R^3} \frac{\partial^3 U}{\partial \theta^3} + \frac{l^3 \mu h}{4R} \frac{\partial^3 U}{\partial \theta \partial x^2} + \frac{3l^2 \mu h}{4R} \frac{\partial \psi_\theta}{\partial x} - \frac{l^2 \mu h}{4} \frac{\partial^3 V}{\partial x^3} \right) R d\theta \Big|_0^L = 0 \quad \text{Or} \quad \delta V \Big|_{x=0,L} = 0, \quad (38)$$

$$\int_0^{2\pi} \left(-\frac{l^2 \mu h}{4R} \frac{\partial^2 U}{\partial x \partial \theta} - \frac{l^2 \mu h}{4R^2} \frac{\partial W}{\partial \theta} - \frac{l^2 \mu h}{4R} \psi_\theta + \frac{l^2 \mu h}{4R^2} V + \frac{l^2 \mu h}{4} \frac{\partial^2 V}{\partial x^2} \right) R d\theta \Big|_0^L = 0 \quad \text{Or} \quad \delta \left(\frac{\partial V}{\partial x} \right) \Big|_{x=0,L} = 0 \quad (39)$$

$$\int_0^{2\pi} \left(\frac{l^2 \mu h}{R^2} \frac{\partial^2 V}{\partial x \partial \theta} - \frac{3l^2 \mu h}{4R^2} \frac{\partial^3 W}{\partial x \partial \theta^2} + \frac{l^2 \mu h}{4R} \frac{\partial^2 \psi_\theta}{\partial x \partial \theta} + \frac{l^2 \mu h}{4} \frac{\partial^2 \psi_x}{\partial x^2} - \frac{l^2 \mu h}{4} \frac{\partial^3 W}{\partial x^3} - \frac{3l^2 \mu h}{4R^3} \frac{\partial^2 U}{\partial \theta^2} - \frac{3\tilde{e}_{15}}{2\beta} \sin\left(\frac{\beta h}{2}\right) \frac{\partial \phi}{\partial x} + \left(1/4\tilde{c}_{55} h - \frac{l^2 \mu h}{4R^2} \right) \psi_x + \left(\frac{\tilde{c}_{55} h}{4} + \frac{l^2 \mu h}{4R^2} \right) \frac{\partial W}{\partial x} + \frac{l^2 \mu h}{2R^2} \frac{\partial^2 \psi_x}{\partial \theta^2} + \frac{-k_g}{2} \frac{\partial W}{\partial x} \right) R d\theta \Big|_0^L = 0 \quad \text{Or} \quad \delta W \Big|_{x=0,L} = 0, \quad (40)$$

$$\int_0^{2\pi} \left(\frac{l^2 \mu h}{4R^2} \frac{\partial V}{\partial \theta} - \frac{l^2 \mu h}{4R^2} \frac{\partial^2 W}{\partial \theta^2} + \frac{l^2 \mu h}{4R} \frac{\partial \psi_\theta}{\partial \theta} - \frac{l^2 \mu h}{4} \frac{\partial \psi_x}{\partial x} + \frac{l^2 \mu h}{4} \frac{\partial^2 W}{\partial x^2} + \frac{k_g}{2} W \right) R d\theta \Big|_0^L = 0 \quad \text{Or} \quad \delta \left(\frac{\partial W}{\partial x} \right) \Big|_{x=0,L} = 0, \quad (41)$$

$$\int_0^{2\pi} \left(-\frac{l^2 \mu h}{4R^2} \frac{\partial V}{\partial \theta} + \frac{l^2 \mu h}{4R^2} \frac{\partial^2 W}{\partial \theta^2} - \frac{l^2 \mu h}{4} \frac{\partial^2 W}{\partial x^2} + \left(\frac{\tilde{c}_{11} h^3}{12} + \frac{l^2 \mu h}{4} \right) \frac{\partial \psi_x}{\partial x} - \frac{l^2 \mu h}{4R} \frac{\partial \psi_\theta}{\partial \theta} + \tilde{e}_{31} \beta \left(-\frac{h}{\beta} \cos\left(\frac{\beta h}{2}\right) + \frac{2}{\beta^2} \sin\left(\frac{\beta h}{2}\right) \right) \phi \right) R d\theta \Big|_0^L = 0 \quad \text{Or} \quad \delta \psi_x \Big|_{x=0,L} = 0, \quad (42)$$

$$\int_0^{2\pi} \left(\frac{-l^2 \mu h^3}{48} \frac{\partial^3 \psi_\theta}{\partial x^3} + \frac{l^2 \mu h}{2R} \frac{\partial V}{\partial x} + \frac{l^2 \mu h}{2R^2} \frac{\partial U}{\partial \theta} - \frac{l^2 \mu h}{2R} \frac{\partial^2 W}{\partial x \partial \theta} + \left(\frac{\tilde{c}_{66} h^3}{48} + l^2 \mu h \right) \frac{\partial \psi_\theta}{\partial x} - \frac{l^2 \mu h}{2R} \frac{\partial \psi_x}{\partial \theta} \right) R d\theta \Big|_0^L = 0 \quad \text{Or} \quad \delta \psi_\theta \Big|_{x=0,L} = 0, \quad (43)$$

$$\int_0^{2\pi} \left(\frac{l^2 \mu h^3}{48} \frac{\partial^2 \psi_\theta}{\partial x^2} \right) R d\theta \Big|_0^L = 0 \quad \text{Or} \quad \delta \left(\frac{\partial \psi_\theta}{\partial x} \right) \Big|_{x=0,L} = 0, \quad (44)$$

$$\int_0^{2\pi} \left(\frac{-3\tilde{e}_{15}}{2\beta} \sin\left(\frac{\beta h}{2}\right) \frac{\partial W}{\partial x} - \frac{3\tilde{e}_{15}}{2\beta} \sin\left(\frac{\beta h}{2}\right) \psi_x - \frac{\tilde{s}_{11}}{2\beta} \left(2\cos\left(\frac{\beta h}{2}\right) \sin\left(\frac{\beta h}{2}\right) + \beta h \right) \frac{\partial \phi}{\partial x} \right) R d\theta \Big|_0^L = 0$$

$$\text{Or} \quad \delta \phi \Big|_{x=0,L} = 0. \quad (45)$$

The boundary conditions in the constant θ case are as follow:

$$\int_0^L \left(\left(\frac{\tilde{c}_{66} h}{4R^2} + \frac{l^2 \mu h}{R^4} \right) \frac{\partial U}{\partial \theta} + \left(-\frac{l^2 \mu h}{4R^3} + \frac{c_{66} h}{4R} \right) \frac{\partial V}{\partial x} + \frac{l^2 \mu h}{4R} \frac{\partial^3 V}{\partial x^3} + \frac{l^2 \mu h}{4R^2} \frac{\partial \psi_\theta}{\partial x} - \frac{l^2 \mu h}{4R^2} \frac{\partial^3 U}{\partial x^2 \partial \theta} + \right.$$

$$\left. \frac{l^2 \mu h}{2R^3} \frac{\partial^2 W}{\partial x \partial \theta} - \frac{l^2 \mu h}{R^3} \frac{\partial \psi_x}{\partial \theta} \right) R d x \Big|_0^{2\pi} = 0 \quad \text{Or} \quad \delta U \Big|_{\theta=0,2\pi} = 0, \quad (46)$$

$$\int_0^L \left(-\frac{l^2 \mu h}{4R^3} \frac{\partial W}{\partial x} + \frac{l^2 \mu h}{4R^3} \psi_x - \frac{l^2 \mu h}{4R^3} \frac{\partial^2 V}{\partial x \partial \theta} + \frac{l^2 \mu h}{4R^4} \frac{\partial^2 U}{\partial \theta^2} \right) R d x \Big|_0^{2\pi} = 0 \quad \text{Or} \quad \delta \left(\frac{\partial U}{\partial \theta} \right) \Big|_{\theta=0,2\pi} = 0, \quad (47)$$

$$\int_0^L \left(\frac{-l^2 \mu h}{4R^2} \frac{\partial^3 V}{\partial x^2 \partial \theta} + \frac{l^2 \mu h}{4R^3} \frac{\partial^3 U}{\partial \theta^2 \partial x} - \frac{l^2 \mu h}{4R^4} \frac{\partial^2 W}{\partial \theta^2} + \frac{l^2 \mu h}{4R^3} \frac{\partial \psi_\theta}{\partial \theta} + \left(\frac{\tilde{c}_{22} h}{R^2} + \frac{l^2 \mu h}{4R^4} \right) \frac{\partial V}{\partial \theta} + \right.$$

$$\left. \frac{\tilde{c}_{12} h}{R} \frac{\partial U}{\partial x} + \frac{\tilde{c}_{22} h}{R^2} W \right) R d x \Big|_0^{2\pi} = 0 \quad \text{Or} \quad \delta V \Big|_{\theta=0,2\pi} = 0, \quad (48)$$

$$\int_0^L \left[\left(\frac{3l^2 \mu h}{4R^2} \frac{\partial^2 V}{\partial x^2} - \frac{3l^2 \mu h}{4R^2} \frac{\partial^3 W}{\partial x^2 \partial \theta} - \frac{l^2 \mu h}{4R^3} \frac{\partial^2 U}{\partial x \partial \theta} + \frac{l^2 \mu h}{2R} \frac{\partial^2 \psi_\theta}{\partial x^2} + \frac{l^2 \mu h}{4R^2} \frac{\partial^2 \psi_x}{\partial x \partial \theta} + \frac{l^2 \mu h}{4R^3} \frac{\partial^2 \psi_\theta}{\partial \theta^2} - \right. \right.$$

$$\left. \frac{l^2 \mu h}{4R^4} \frac{\partial^3 W}{\partial \theta^3} + \frac{l^2 \mu h}{4R^4} \frac{\partial^2 V}{\partial \theta^2} - \frac{3\tilde{e}_{24}}{2R^2 \beta} \sin\left(\frac{\beta h}{2}\right) \frac{\partial \phi}{\partial \theta} + \left(\frac{\tilde{c}_{44} h}{4R} + \frac{l^2 \mu h}{4R^3} \right) \psi_\theta - \left(\frac{\tilde{c}_{44} h}{4R^2} + \frac{l^2 \mu h}{4R^4} \right) V + \right.$$

$$\left. \left(\frac{\tilde{c}_{44} h}{4R^2} + \frac{l^2 \mu h}{4R^4} \right) \frac{\partial W}{\partial \theta} + \frac{-k_g}{2R^2} \frac{\partial W}{\partial \theta} \right) R d x \Big|_0^{2\pi} = 0 \quad \text{Or} \quad \delta W \Big|_{\theta=0,2\pi} = 0, \quad (49)$$

$$\int_0^L \left(\frac{-l^2 \mu h}{4R^2} \frac{\partial^2 W}{\partial x^2} - \frac{l^2 \mu h}{4R^3} \frac{\partial \psi_\theta}{\partial \theta} + \frac{l^2 \mu h}{4R^2} \frac{\partial \psi_x}{\partial x} + \frac{l^2 \mu h}{4R^4} \frac{\partial^2 W}{\partial \theta^2} - \frac{l^2 \mu h}{4R^4} \frac{\partial V}{\partial \theta} + \frac{k_g}{2R^2} W \right) R d x \Big|_0^{2\pi} = 0$$

$$\text{Or} \quad \delta \left(\frac{\partial W}{\partial \theta} \right) \Big|_{\theta=0,2\pi} = 0, \quad (50)$$

$$\int_0^L \left(\frac{l^2 \mu h}{2R^2} \frac{\partial V}{\partial x} - \frac{l^2 \mu h}{R^3} \frac{\partial U}{\partial \theta} - \frac{l^2 \mu h}{2R^2} \frac{\partial^2 W}{\partial x \partial \theta} - \frac{l^2 \mu h}{2R} \frac{\partial \psi_\theta}{\partial x} + \frac{l^2 \mu h}{R^2} \frac{\partial \psi_x}{\partial \theta} \right) R dx \Big|_0^{2\pi} = 0$$

Or $\delta \psi_x \Big|_{\theta=0, 2\pi} = 0,$

$$\int_0^L \left(\frac{l^2 \mu h}{4R^3} \frac{\partial V}{\partial \theta} - \frac{l^2 \mu h}{4R^3} \frac{\partial^2 W}{\partial \theta^2} + \frac{l^2 \mu h}{4R} \frac{\partial^2 W}{\partial x^2} - \frac{l^2 \mu h}{4R} \frac{\partial \psi_x}{\partial x} + \frac{l^2 \mu h}{4R^2} \frac{\partial \psi_\theta}{\partial \theta} \right) R dx \Big|_0^{2\pi} = 0$$

Or $\delta \psi_\theta \Big|_{\theta=0, 2\pi} = 0,$

$$\int_0^L \left(\frac{-3\tilde{e}_{24}}{2R^2 \beta} \sin\left(\frac{\beta h}{2}\right) \frac{\partial W}{\partial \theta} - \frac{3\tilde{e}_{24}}{2R\beta} \sin\left(\frac{\beta h}{2}\right) \psi_\theta + \frac{3\tilde{e}_{24}}{2R^2 \beta} \sin\left(\frac{\beta h}{2}\right) V \right. \\ \left. - \frac{\tilde{s}_{22}}{2R^2 \beta} \left(2\cos\left(\frac{\beta h}{2}\right) \sin\left(\frac{\beta h}{2}\right) + \beta h \right) \frac{\partial \phi}{\partial \theta} \right) R dx \Big|_0^{2\pi} = 0 \quad \text{Or} \quad \delta \phi \Big|_{\theta=0, 2\pi} = 0.$$

3. Governing equations of simply supported piezoelectric cylindrical shell

In the present work, the essential and natural boundary conditions corresponding to simply support are as follows:

$$V \Big|_{x=0, L} = 0 \tag{54}$$

$$W \Big|_{x=0, L} = 0 \tag{55}$$

$$\phi \Big|_{x=0, L} = 0 \tag{55}$$

$$\left(\tilde{c}_{11} h \frac{\partial U}{\partial x} + \left(\frac{l^2 \mu h}{4R^3} + \frac{\tilde{c}_{12} h}{R} \right) \frac{\partial V}{\partial \theta} + \frac{l^2 \mu h}{4R} \frac{\partial^3 V}{\partial \theta \partial x^2} - \frac{l^2 \mu h}{4R^3} \frac{\partial^2 W}{\partial \theta^2} - \frac{l^2 \mu h}{4R^2} \frac{\partial \psi_\theta}{\partial \theta} - \frac{l^2 \mu h}{4R^2} \frac{\partial^3 U}{\partial \theta^2 \partial x} + \frac{\tilde{c}_{12} h}{R} W \right) \Big|_{x=0, L} = 0, \tag{56}$$

$$\left(-\frac{l^2 \mu h}{4R} \frac{\partial^2 U}{\partial x \partial \theta} - \frac{l^2 \mu h}{4R^2} \frac{\partial W}{\partial \theta} - \frac{l^2 \mu h}{4R} \psi_\theta + \frac{l^2 \mu h}{4R^2} V + \frac{l^2 \mu h}{4} \frac{\partial^2 V}{\partial x^2} \right) \Big|_{x=0, L} = 0, \tag{57}$$

$$\left(\frac{l^2 \mu h}{4R^2} \frac{\partial V}{\partial \theta} - \frac{l^2 \mu h}{4R^2} \frac{\partial^2 W}{\partial \theta^2} + \frac{l^2 \mu h}{4R} \frac{\partial \psi_\theta}{\partial \theta} - \frac{l^2 \mu h}{4} \frac{\partial \psi_x}{\partial x} + \frac{l^2 \mu h}{4} \frac{\partial^2 W}{\partial x^2} + \frac{k_g}{2} W \right) \Big|_{x=0, L} = 0, \tag{58}$$

$$\left(-\frac{l^2 \mu h}{4R^2} \frac{\partial V}{\partial \theta} + \frac{l^2 \mu h}{4R^2} \frac{\partial^2 W}{\partial \theta^2} - \frac{l^2 \mu h}{4} \frac{\partial^2 W}{\partial x^2} + \left(\frac{\tilde{c}_{11} h^3}{12} + \frac{l^2 \mu h}{4} \right) \frac{\partial \psi_x}{\partial x} \right) \bigg|_{x=0,L} = 0, \quad (59)$$

$$\left(-\frac{l^2 \mu h}{4R} \frac{\partial \psi_\theta}{\partial \theta} + \tilde{e}_{31} \beta \left(-\frac{h}{\beta} \cos\left(\frac{\beta h}{2}\right) + \frac{2}{\beta^2} \sin\left(\frac{\beta h}{2}\right) \right) \phi \right) \bigg|_{x=0,L} = 0,$$

$$\left(\frac{-l^2 \mu h^3}{48} \frac{\partial^3 \psi_\theta}{\partial x^3} + \frac{l^2 \mu h}{2R} \frac{\partial V}{\partial x} + \frac{l^2 \mu h}{2R^2} \frac{\partial U}{\partial \theta} - \frac{l^2 \mu h}{2R} \frac{\partial^2 W}{\partial x \partial \theta} + \left(\frac{\tilde{c}_{66} h^3}{48} + l^2 \mu h \right) \frac{\partial \psi_\theta}{\partial x} - \frac{l^2 \mu h}{2R} \frac{\partial \psi_x}{\partial \theta} \right) \bigg|_{x=0,L} = 0. \quad (60)$$

4. Navier method for simply supported end conditions

As nanoshell is assumed to have simple support, Navier solution is used to solve the equations of motion and boundary conditions.

The Navier solution corresponds to the current work considering the field variables as below:

$$\begin{aligned} U(x, \theta, t) &= \sum_n \sum_m U_{mn}(t) \cos\left(\frac{m\pi x}{L}\right) \cos(n\theta) \\ V(x, \theta, t) &= \sum_n \sum_m V_{mn}(t) \sin\left(\frac{m\pi x}{L}\right) \sin(n\theta) \\ W(x, \theta, t) &= \sum_n \sum_m W_{mn}(t) \sin\left(\frac{m\pi x}{L}\right) \cos(n\theta) \\ \phi(x, \theta, t) &= \sum_n \sum_m \phi_{mn}(t) \sin\left(\frac{m\pi x}{L}\right) \cos(n\theta) \\ \psi_x(x, \theta, t) &= \sum_n \sum_m \psi_{mn}(t) \cos\left(\frac{m\pi x}{L}\right) \cos(n\theta) \\ \psi_\theta(x, \theta, t) &= \sum_n \sum_m \psi_{mn}(t) \sin\left(\frac{m\pi x}{L}\right) \sin(n\theta) \end{aligned} \quad (61)$$

Where m and n are the axial and circumferential wave numbers, respectively. $U_{mn}(t)$, $V_{mn}(t)$, $W_{mn}(t)$, $\phi_{mn}(t)$ and $\psi_{mn}(t)$ are the generalized unknown functions of t .

By substituting Eq. (61) into the equations of motion, the equations are written in the matrix form as follows:

$$[k]\{d\} + [M]\{\ddot{d}\} = 0 \quad (62)$$

Where,

$$\{d\} = \{d_0\} e^{i\omega x} \quad (63)$$

Now by substituting Eq. (63) into (62), we have:

$$([k] - \omega^2 [M])\{d_0\} = 0 \quad (64)$$

Where ω is the natural frequency and $\{d_0\} = \{U_{mn}, V_{mn}, W_{mn}, \phi_{mn}, \psi_{mn}\}^T$ is the displacement amplitude vector.

5. Results and discussion

At first comparison, a study is carried out to guarantee the presented result and used method. So the results for a nanoshell are computed and listed in Table 1, also the corresponding results presented in a paper by Zeighampour and Tadi Beni [16] are prepared and listed. They analyze the free vibration of a thin shell based on classical shell theory. For the nanoscale size effect, they used the modified strain gradient theory. For this case, the natural frequency is defined as:

$$\Omega = \omega R \sqrt{\rho / E} \quad (65)$$

And the radius of the nanoshell is:

$$R = 2.32 \text{ nm}$$

In Table 1, the natural frequency parameters for two cases, $h/R = 0.02$ and $h/R = 0.05$ are presented.

Table 1 shows a good agreement between the present result and those presented by Zeighampour and Tadi Beni [16]. Also for the certainty of the piezoelectric formulation of the present work, the results are compared with a piezoelectric nanoshell modeled by Ke et al [21]. These results are shown in Table 2.

Table 1. Comparison of natural frequency parameters for a simply supported isotropic nanoshell.

	$h/R = 0.02$			$h/R = 0.05$		
	$l = 0$	$l = h$	Reference[16]	$l = 0$	$l = h$	Reference[16]
ω_{11}	0.1954	0.1954	0.19686	0.1954	0.1957	0.20036
ω_{22}	0.2527	0.2568	0.25632	0.2589	0.2827	0.2633
ω_{33}	0.2758	0.3051	0.27730	0.3141	0.4499	0.31577
ω_{44}	0.3916	0.3916	0.30178	0.4143	0.7409	0.40671
ω_{55}	0.3420	0.5298	0.34375	0.5672	1.1389	0.55360

Table 2. Comparison of natural frequency parameters for a piezoelectric nanoshell.

m	Present study	Reference [21]
2	0.5873	0.6192
3	1.2182	1.2366
4	1.9624	1.9775
5	2.7502	2.7660
6	3.5323	3.5508

For this case, the geometrical dimensions of the nanoshell are:

$$h = 1nm$$

$$R = 50h$$

$$L = 12R$$

And the properties of PZT-4 that are used are shown in Table 3.

Table 3. PZT-4 properties

Elastic (GPa)	$c_{11} = 139$ $c_{12} = 77.8$ $c_{13} = 74$ $c_{22} = 139$ $c_{23} = 74$ $c_{33} = 115$ $c_{44} = 25.6$ $c_{66} = 30.6$
Piezoelectric (C / m^2)	$e_{15} = 12.7$ $e_{24} = 12.7$ $e_{31} = -5.2$ $e_{32} = -5.2$ $e_{33} = 15.1$
Dielectric ($10^{-9} C / Vm$)	$s_{11} = 6.46$ $s_{22} = 6.46$ $s_{33} = 5.62$

As shown in Table 2, it is obvious that the present results for the piezoelectric case are very close to the results of Ke et al. [21].

After the comparison study, the results of piezoelectric nanoshell conveying fluid are presented.

The geometrical and physical parameters are as below:

$$R = 1nm, \quad H = 0.5R, \quad k_w = 1 \times 10^5, \quad \rho_t = 2300kg / m^3, \quad l = h,$$

$$L = 15R, \quad C_d = 1 \times 10^5, \quad k_g = 0.75, \quad \rho_f = 1000kg / m^3, \quad v_f = 20m / s.$$

Except for other values that are mentioned for each figure or table, the above values are used for all cases. Figs 2 and 3 show the imaginary (natural frequency) and real (damping) of piezoelectric nanoshell L / R s vs ratio for various k_g . As shown in these figures, it is found that both natural frequency and damping are decreased by

increasing the L/R ratio. Moreover, by increasing k_g , the real part (damping) decreases, and the imaginary part (frequency) increases. This result is expected because k_g has no contribution to global damping and mass of the system and only appears in the global stiffness of the system. The normal consequence is the reduction in damping and an increase in frequency of the system with k_g . Additionally, by increasing the length of nanoshell, the general stiffness of the system decreases causing the frequency of the system to reduce. This conclusion can more obviously be seen in Fig. 4. In this figure, first three natural frequency parameters for $n=1$ and $m=1,2$ and 3 are plotted versus L/R ratio. It is observed that all three frequency parameters decrease by increasing the L/R ratio.

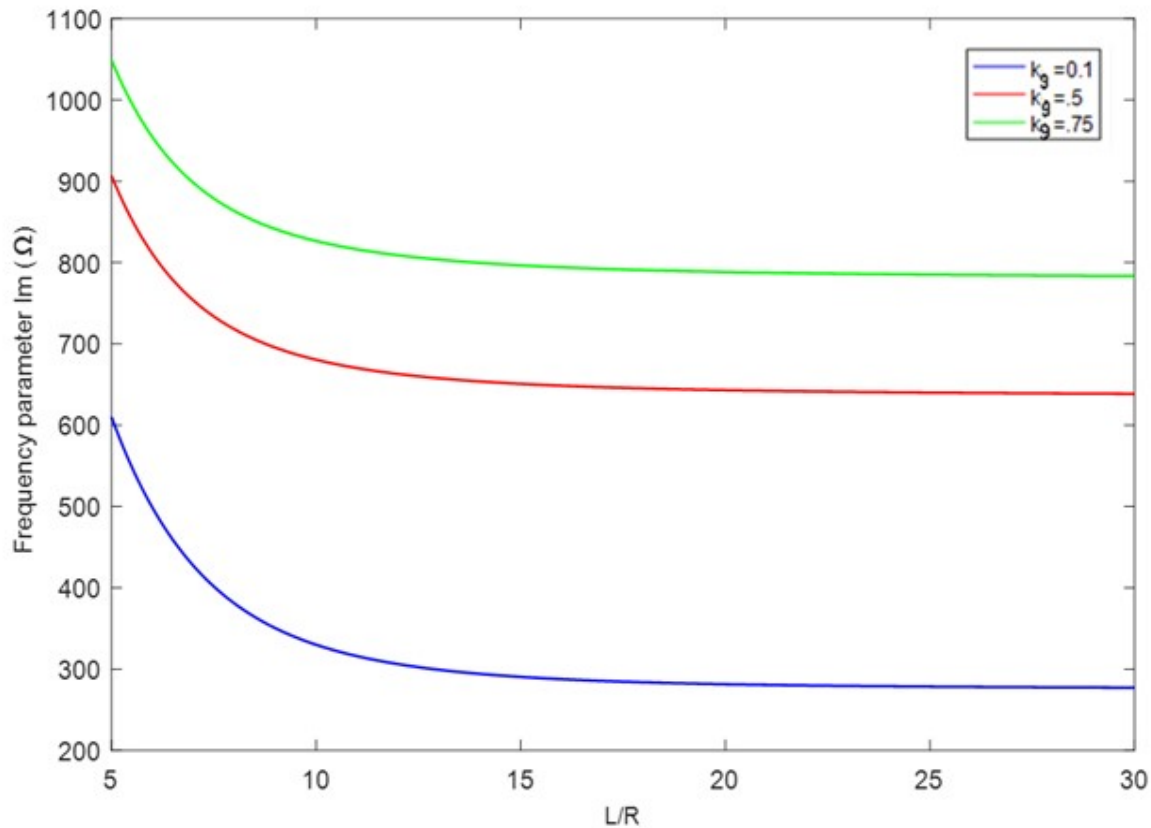


Fig.2. The imaginary part of frequency parameter versus L/R ratio for various k_g .

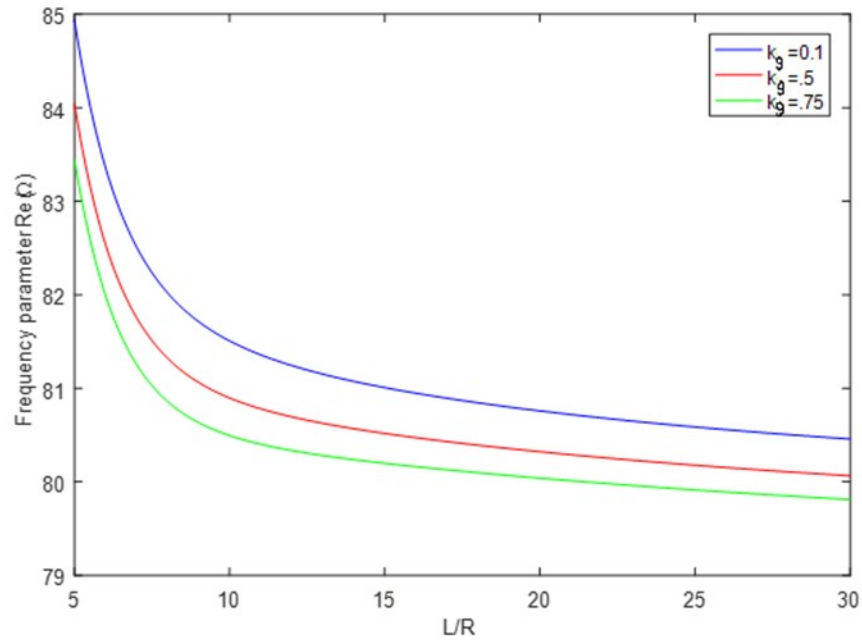


Fig.3. Real part of frequency parameter versus L / R ratio for various k_g

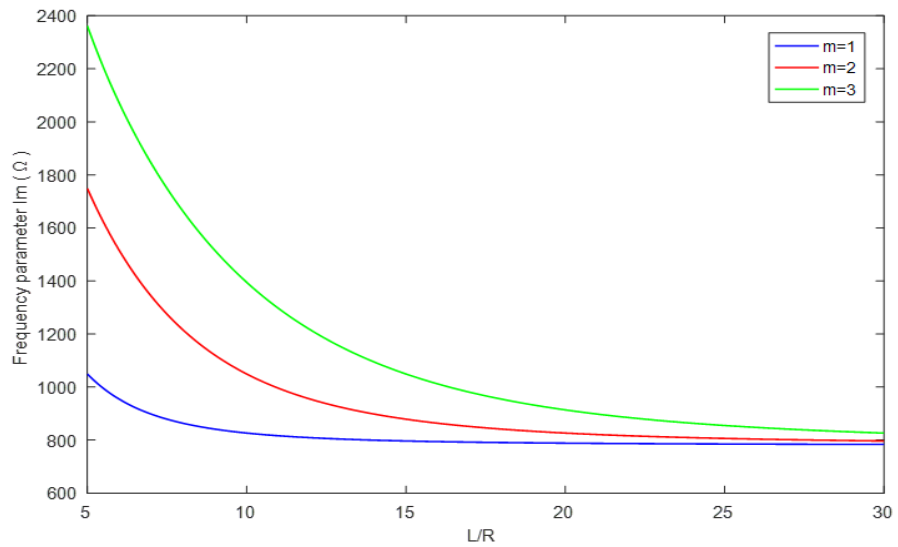


Fig.4. Imaginary part of frequency parameter versus L / R ratio for various m

Figure 5, shows the frequency parameter versus the thickness-to-radius ratio of piezoelectric nanoshells for various size effect parameters. This figure shows that for small thicknesses, the size effect parameter causes no important difference in frequency parameter and only for large amounts of thicknesses does the size effect parameter make considerable difference. It should be mentioned that the size effect parameter is directly connected to the thickness of the nanoshell so by increasing the thickness of the nanoshell, the size effect parameter directly increases and consequently the effect of the size effect parameter increases. Moreover, for more resolution, the effect of the size effect parameter is presented in Table 4. In this table, first three frequency parameters for nanoshells with various size effect parameters are presented. As can be seen in this table, the size effect parameter of a small value has no considerable effect on frequency parameters and only for very large values of size effects parameters (about $l = 100h$) we can see the size effect differences in frequency parameters as shown in fig 4. Also, Fig. 6 shows the positive and negative parts of the frequency parameter. As can be seen in the figure, the frequency parameter approaches a constant value as the effect of the size of the virtual part increases.

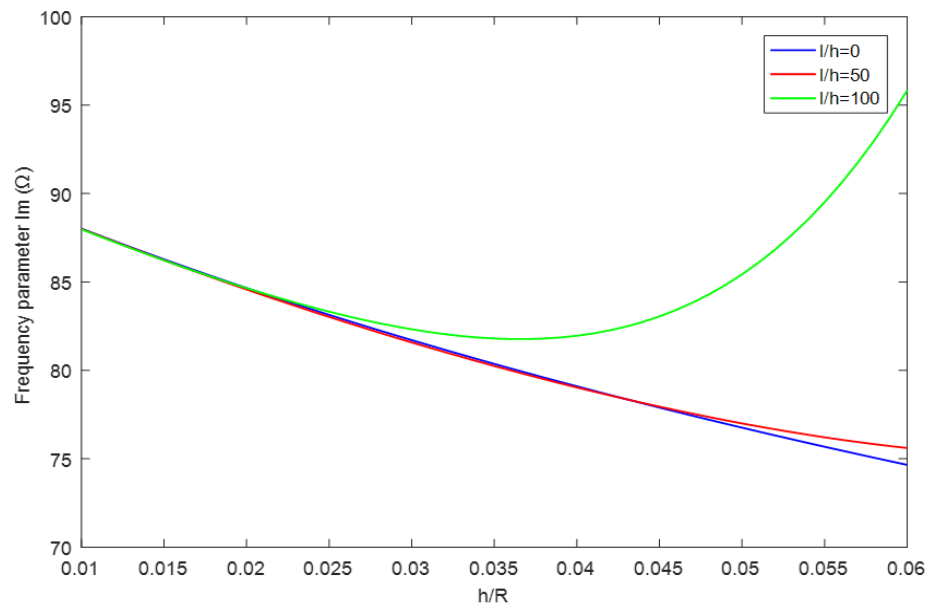


Fig.5. Imaginary part of frequency parameter versus h / R ratio for various l / h

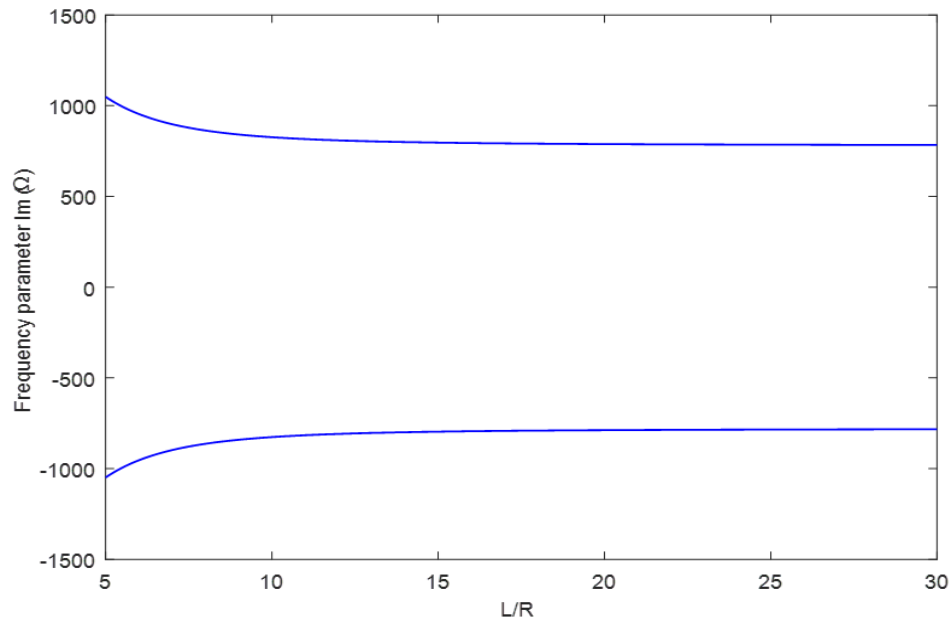


Fig.6. positive and negative parts of the frequency parameter

The effects of nonviscous fluid on frequency and damping parameters are presented in Figs 6 and 7. In these figures, the frequency and damping parameters are plotted versus dimensionless flow velocity. This figure shows that the real part of the frequency parameter (damping) of the system increase linearly with increasing the flow velocity and the imaginary part (frequency) decreases by increasing the flow velocity. This result can be justified by consideration of the fact that the flow velocity has a damping effect on the system.

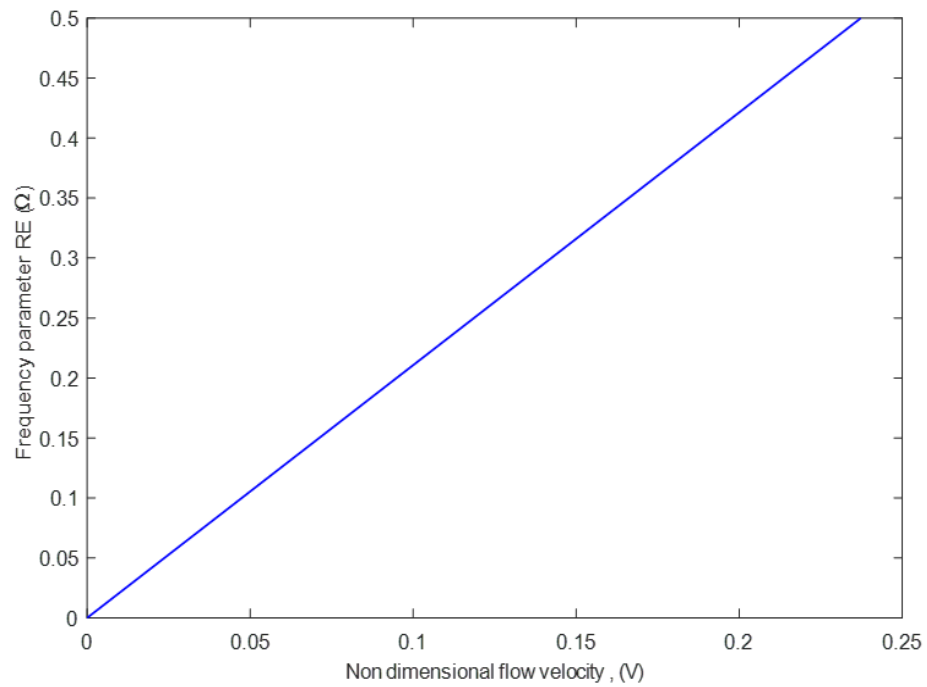


Fig.7. Real part of frequency parameters versus dimensionless flow velocity.

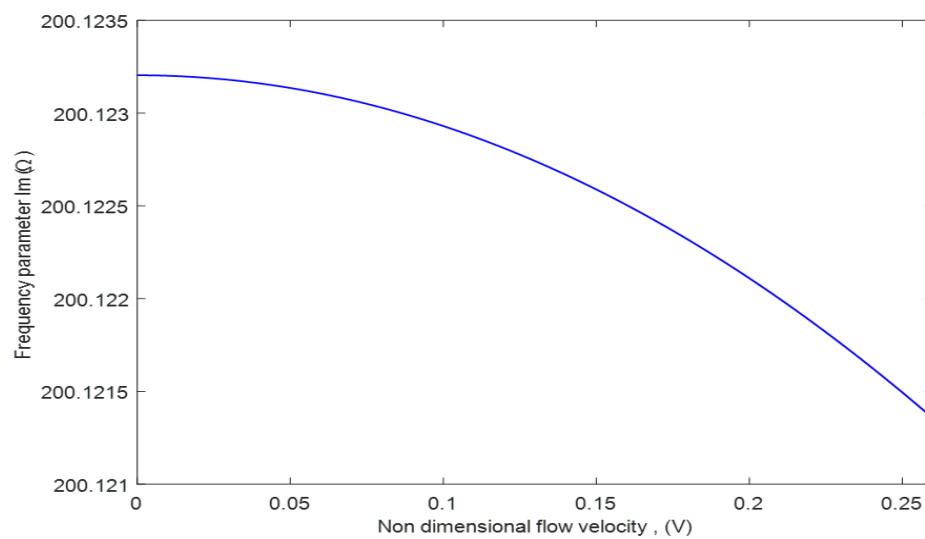


Fig.8. Imaginary part of frequency parameters versus flow velocity

Table 4. First tree frequency parameters for nanoshell with various size effect parameters l and $m = n = 1$

	$h/R = 0.01$			$h/R = 0.05$		
	$l = 0$	$l = h$	$l = 10h$	$l = 0$	$l = h$	$l = 10h$
Ω_1	1155.18	1155.18	1155.16	199.14	199.14	198.74
Ω_2	3624.11	3624.32	3624.15	731.11	732.03	799.15
Ω_3	6368.44	6368.52	6376.19	1353.35	1353.77	1392.41

Table 5. First tree frequency parameters for nanoshell with $h/R = 0.05$, for various C_d , $m = n = 1$

	$C_g = 0$	$C_d = 1 \times 10^5$	$C_d = 1 \times 10^6$
Ω_1	200.12	199.67	151.83
Ω_2	732.16	732.05	731.02
Ω_3	1353.89	1353.84	1348.86

Finally, to show the effects of damping coefficient on the system frequency parameters, the results for a piezoelectric nanoshell for various damping coefficients are prepared in table 6. The natural frequency parameter decreases by increasing damping coefficient.

4. Conclusions

Free vibration analysis of piezoelectric nanoshells is performed based on the first-order shear deformation theory. The nanoscale size effect is imposed according to the couple stress theory and the Navier method is used to solve the free vibration problem.

Some conclusions are as follows:

1. The size effect parameters have a considerable effect on natural frequency only for large values of it.
2. Both natural frequency and damping parameters decrease by increasing the length of the nanoshell.
3. By increasing the Pasternak constant k_g , the natural frequency is increased and the damping of the system decreased.
4. The flow velocity act as a damper for the nanoshell and by increasing the flow velocity, the frequency of the system is decreased and the damping of the system increased.

Appendix A:

$$k = \frac{\mu l^2}{2}$$

$$A_1 = \frac{kh}{8R^4}; A_2 = -\frac{kh}{8R^3}; A_3 = -\frac{kh}{4R^3}; A_4 = \frac{5kh}{8R^3}; A_5 = -\frac{kh}{8R^2}; A_6 = -(\frac{\tilde{C}_{66}h}{R^2} + \frac{kh}{2R^4});$$

$$A_7 = -\tilde{C}_{11}h; A_8 = \frac{kh}{8R^3} - \frac{\tilde{C}_{12}h}{R} - \frac{\tilde{C}_{66}h}{R}; A_9 = -\frac{\tilde{C}_{12}h}{R}; A_{10} = -\rho_l h$$

$$B_1 = \frac{3kh}{8R^2}; B_2 = -(\frac{kh}{4R^2} + \tilde{C}_{66}h); B_3 = -\frac{3kh}{4R}; B_4 = \frac{kh}{8R^4}; B_5 = -(\frac{\tilde{C}_{11}h}{R^2} + \frac{kh}{8R^4});$$

$$B_6 = -\frac{kh}{8R^3}; B_7 = -\frac{kh}{4R^2}; B_8 = -(\frac{\tilde{C}_{11}h}{R^2} + \frac{\tilde{C}_{44}h}{R^2} + \frac{kh}{8R^4}); B_9 = -(\frac{\tilde{C}_{44}h}{R} + \frac{kh}{8R^3});$$

$$B_{10} = \frac{\tilde{C}_{44}h}{R^2} + \frac{kh}{8R^4}; B_{11} = -\frac{\tilde{C}_{12}h}{R} - \frac{\tilde{C}_{66}h}{R} + \frac{kh}{8R^3}; B_{12} = \frac{kh}{8}; B_{13} = -\frac{kh}{8R};$$

$$B_{14} = \frac{kh}{8R^2}; B_{15} = -\frac{kh}{8R^3}; B_{16} = \frac{2e_{24}h}{\pi R^2}; B_{17} = -\rho_t h;$$

$$E_1 = \frac{kh}{4R^2}; E_2 = -\frac{3kh}{8R^2}; E_3 = -\frac{kh}{8R}; E_4 = \frac{kh}{8R^4}; E_5 = -\frac{kh}{8R^4}; E_6 = -\frac{kh}{8R^3}; E_7 = -\frac{kh}{8R^2};$$

$$E_8 = \frac{kh}{8}; E_9 = -\frac{kh}{8}; E_{10} = -(\frac{\tilde{C}_{44}h}{R^2} + \frac{kh}{8R^4} + \frac{k_g}{R^2}); E_{11} = -(\frac{\tilde{C}_{44}h}{R} + \frac{kh}{8R^3});$$

$$E_{12} = \frac{\tilde{C}_{44}h}{R^2} + \frac{\tilde{C}_{11}h}{R^2} + \frac{kh}{8R^4}; E_{13} = \frac{kh}{4R^3}; E_{14} = -(\tilde{C}_{55}h + \frac{kh}{8R^2} + k_g - \frac{\rho_f v_f^2 R}{2});$$

$$E_{15} = -\tilde{C}_{55}h + \frac{kh}{8R^2}; E_{16} = \frac{\tilde{C}_{12}h}{R}; E_{17} = \frac{\tilde{C}_{11}h}{R^2} + k_w; E_{18} = \frac{2\tilde{e}_{24}h}{\pi R^2}; E_{19} = \frac{2\tilde{e}_{15}h}{\pi};$$

$$E_{20} = \frac{2v_0\tilde{e}_{32}}{R}; E_{21} = \rho_f v_f R; E_{22} = C_d; E_{23} = -(\frac{\rho_f R}{2} + \rho_l h);$$

$$C_1 = \frac{kh}{8R^2}; C_2 = \frac{-kh}{4R^2}; C_3 = -(\frac{\tilde{C}_{12}h^4}{12R} + \frac{\tilde{C}_{66}h^5}{12R} - \frac{3kh^3}{8R}); C_4 = \frac{kh}{8}; C_5 = -(\frac{\tilde{C}_{11}h^3}{12} + \frac{kh}{8});$$

$$C_6 = -(\frac{kh}{2R^2} + \frac{\tilde{C}_{66}h^3}{12R^2}); C_7 = \frac{5kh}{8R^3}; C_8 = -\frac{kh}{8R^2} + \tilde{C}_{55}h; C_9 = \frac{kh}{8R^2} + \tilde{C}_{55}h;$$

$$C_{10} = -(\frac{2\tilde{e}_{15}h}{\pi} + \frac{2\tilde{e}_{13}h}{\pi}); C_{11} = -\frac{\rho_l h^3}{12};$$

$$\begin{aligned}
D_1 &= \frac{kh}{8R}; D_2 = \frac{-3kh}{8R}; D_3 = -\left(\frac{\tilde{C}_{66}h^3}{12} + \frac{kh}{2} + \frac{kh^3}{48R^2}\right); D_4 = \frac{kh}{8R^3}; D_5 = -\frac{kh}{8R^3}; \\
D_6 &= -\left(\frac{kh}{8R^2} + \frac{\tilde{C}_{11}h^3}{12R^2}\right); D_7 = -\left(\frac{\tilde{C}_{12}h^3}{12R} + \frac{\tilde{C}_{66}h^3}{12R} - \frac{3kh}{8R}\right); D_8 = \frac{kh}{8R^3} + \frac{\tilde{C}_{44}h}{R}; \\
D_9 &= \tilde{C}_{44}h + \frac{kh}{8R^2}; D_{10} = -\left(\frac{kh}{8R^3} + \frac{\tilde{C}_{44}h}{R}\right); D_{11} = -\frac{kh}{8R^2}; D_{12} = -\frac{kh^3}{96}; \\
D_{13} &= -\left(\frac{2\tilde{e}_{32}h}{\pi R} + \frac{2\tilde{e}_{24}h}{\pi R}\right); D_{14} = -\frac{\rho_i h^3}{12}; \\
F_1 &= \frac{2\tilde{e}_{15}h}{\pi} + \frac{2\tilde{e}_{31}h}{\pi}; F_2 = \left(\frac{2\tilde{e}_{32}h}{\pi R} + \frac{2\tilde{e}_{24}h}{\pi R}\right); F_3 = \frac{2\tilde{e}_{24}h}{\pi R^2}; F_4 = -\frac{2\tilde{e}_{24}h}{\pi R^2}; F_5 = \frac{2\tilde{e}_{15}h}{\pi}; \\
F_6 &= \frac{s_{11}h}{2R}; F_7 = \frac{s_{22}h}{2R^2}; F_8 = \frac{s_{33}\pi^2}{2h}
\end{aligned}$$

References

- [1] Park J.I., Saffari A., Kumar S., Guñther A., Kumacheva E., 2010. Microfluidic synthesis of polymer and inorganic particulate materials. *Annual Review of Materials Research*. 40, 415–443.
- [2] Li L., Ismagilov R.F. 2010. Protein crystallization using microfluidic technologies based on valves, droplets, and slipchip', *Annu. Rev. Biophys.* 39, 139–158.
- [3] Zhou J.H., Zeng J., Grant J., Wu H.K., Xia Y.N., 2011. On-chip screening of experimental conditions for the synthesis of noble-metal nanostructures with different morphologies. *Small*. 7(23), 3308–16.
- [4] Fleck N.A., Muller G.M., Ashby M.F., Hutchinson J.W. 1994. Strain gradient plasticity: theory and experiment. *Acta Metall. Mater.* 42(2), 475–487.
- [5] Ma Q., Clarke D.R., 1995. Size dependent hardness of silver single crystals *Journal of Materials Research*. 10(4), 853–863.
- [6] Stolken J.S., Evans A.G., 1998. Microbend test method for measuring the plasticity length scale. *Acta Mater.* 46, 5109–511.
- [7] Gao, Y., & Bando, Y., 2002. Nanotechnology: Carbon nanothermometer containing gallium. *Nature* 415(6872), 599.
- [8] Hummer, G., Rasaiah, J. C., & Noworyta, J. P., 2001. Water conduction through the hydrophobic channel of a carbon nanotube. *Nature*. 414(6860), 188–90
- [9] Mattia, D., & Gogotsi, Y., 2008. Review: Static and dynamic behavior of liquids inside carbon nanotubes. *Microfluidics and Nanofluidics*. 5(3), 289–305.
- [10] Yin, L., Qian, Q., & Wang, L., 2011. Strain gradient beam model for dynamics of microscale pipes conveying fluid. *Applied Mathematical Modelling*, 35, 2864–2873.
- [11] Ghorbanpourarani, A., Mohammadimehr, M., Arefmanesh, A., Ghasemi, A., 2010. Transverse vibration of short carbon nanotubes using cylindrical shell and beam models. *Proceedings of the Institution of Mechanical Engineers, Part C: Journal of Mechanical Engineering Science*. 224(3), 745–756.
- [12] Xinping, Z., & Lin, W., 2012. Vibration and stability of micro-scale cylindrical shells conveying fluid based on modified couple stress theory. *Micro & Nano letters*. 7(7), 679–684.
- [13] Alibeigloo, A., Shaban, M., 2013. Free vibration analysis of carbon nanotubes by using a three-dimensional theory of elasticity, *Acta Mech.*, 224 1415–1427.
- [14] Zeighampour, H., Tadi Beni, Y., 2014. Analysis of conical shells in the framework of coupled stresses theory. *International Journal of Engineering Science*. 81, 107–122.
- [15] Tadi Beni, Y., Mehralian, F., Razavi, H., 2015. Free vibration analysis of size-dependent shear deformable functionally graded cylindrical shell based on modified couple stress theory. *Composite Structures*. 120, 65–78.
- [16] Zeighampour, H., Tadi Beni, Y., 2014. Cylindrical thin-shell model based on modified strain gradient theory. *International Journal of Engineering Science*. 78, 27–47.
- [17] Bahaadini, R., Hosseini, M., Jamalpoor, A., 2017. Nonlocal and surface effects on the flutter instability of cantilevered nanotubes conveying fluid subjected to follower forces, *Physica B Condensed Matter*. 509, 55–61.
- [18] Chen, C.Q., Shi, Y., Zhang, Y.S., Zhu, J. and Yan, Y.J., 2006. Size dependence of Young's modulus in ZnO nanowires. *Physical Review Letters*. 96(7), 075505
- [19] Stan, G., Ciobanu, C.V., Parthangal, P.M., Cook, R.F., 2007. Diameter-dependent radial and tangential elastic moduli of ZnO nanowires. *Nano Lett. Nano Lett.* 7(12), 3691–3697.
- [20] Agrawal, R., Peng, B., Gdoutos, E.E., Espinosa, H.D., 2008. Elasticity size effects in ZnO nanowires—a combined experimental–computational approach. *Nano Lett.* 8, 3668–74.
- [21] Ke, L.-L., Wang, Y.-S., Reddy, J.N., 2014. Thermo-electro-mechanical vibration of size-dependent piezoelectric cylindrical nanoshells under various boundary conditions. *Composite Structures*. 116, 626–636.
- [22] Kheibari, F., Tadi Beni, Y., 2016. Size-dependent electro-mechanical vibration of single-walled piezoelectric nanotubes using thin shell model. *Materials & Design*. 114, 572–583.